

Data-driven Two Degree-of-Freedom Control for a Micropump and Microneedle Integrated Device for Diabetes Care

Ruoting Yang*, Mingjun Zhang**, and Tzyh-Jong Tarn*

* Department of Electrical and Systems Engineering, Washington University, St. Louis, MO, 63130, USA

e-mail: ryang@wustl.edu, tarn@ese.wustl.edu.

**Department of Mechanical, Aerospace and Biomedical Engineering, University of Tennessee, Knoxville, TN, USA.

email: mjzhang@utk.edu.

Abstract: This paper presents a dynamic model for a micropump and microneedle integrated system for diabetes care. A novel data-driven two degree-of-freedom control mechanism is proposed for regulating blood glucose concentration to shorten regulating time while maintaining the stability of the system in the presence of model uncertainties and unexpected disturbances. Exact feedforward linearization, gain scheduling, and data-driven planning technique are applied to improve regulation performance as well as robustness. Simulation results indicate that the proposed control has great potential in drug delivery problems.

1 Introduction

Diabetes mellitus is a disease in which the patient has difficulty regulating blood glucose. Diabetes may affect the functioning of many physiological systems, causing everything from retinopathy and circulatory problems, to nephropathy and heart disease. While diabetes can be treated with insulin, the dosage of insulin must be strictly regulated - excess insulin can cause hypoglycemia, whereas insufficient insulin can cause hyperglycemia.

Fig. 1 shows a schematic drawing of a insulin infusion microdevice consisting of a piezoelectric micropump, multiple silicon microneedles, an insulin reservoir, a membrane, wireless telemetry, and a remote control component. This control system regulates blood glucose levels by driving the piezoelectric micropump based on glucose sensor measurements. Very generally, sensor readings are passed via wireless telemetry to the controller, which then drives the micropump, causing the release of insulin from the reservoir, through the microneedles into the patient's bloodstream.

The challenges of controller design mainly come from three areas. First, these systems usually have serious nonlinearities, which are poorly estimated by the corresponding linearized systems. Second, the output measurements often have large model uncertainties, disturbances, and slow sampling rates. Third, in the event of an accidental insulin overdose, there is no way to retrieve the insulin to avoid hypoglycemia.

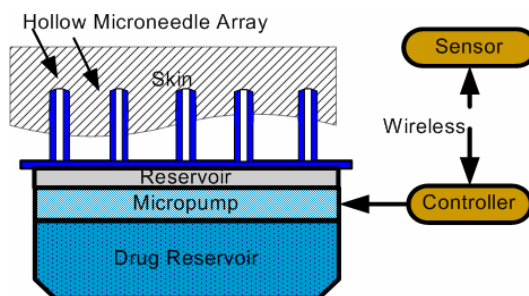


Fig. 1 A schematic drawing of a micropump and microneedle integrated for controlled insulin delivery

Recently, advanced control mechanisms have been applied for glucose control, including PID [1, 2], model predictive control [3, 4], and robust control [5], among others [6]. However, the regulating time that draws the blood glucose concentration from a high level to the basal level is still too long for all these methods. In this paper, we propose a new data-driven feedback and feedforward integrated 2DOF (Two Degree-Of-Freedom) control mechanism to shorten regulating time while maintaining the stability of the system in the presence of model uncertainties and unexpected disturbances. As shown in Fig. 2, the 2DOF control method contains two parts: (1) the feedforward control provides the nominal control to rapidly drive the system towards the desired goal; (2) the feedback control stabilizes the system. It has been proven that the 2DOF controller performs better than controllers that only use feedback under reasonable model uncertainty[7]. The 2DOF control mechanism is said to be time-based if the reference trajectory is given by a time-driven planner. In contrast, a data-driven 2DOF control mechanism

utilizes a data-driven planner to generate the reference trajectory.

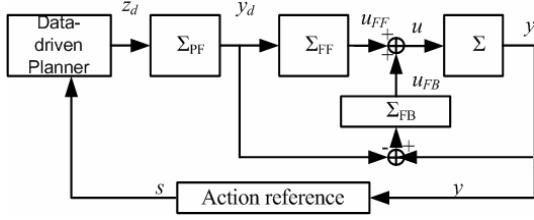


Fig. 2 The schematic of data-driven 2DOF method. Σ_{FF} is the feedforward controller, Σ_{FB} is the feedback controller, and Σ_{PF} is the coordinate transformation between the flat output reference z_d and the output y_d . The data-driven planner is driven by an action reference s generated by the output measurement, instead of driven by time.

The data-driven 2DOF control uses exact feedforward linearization and gain scheduling methods, instead of exact feedback linearization, to improve robustness to model uncertainties, while has the same regulation performance. In addition, we use a data-driven planning technique, which can further improve robustness towards model uncertainties and unexpected disturbances in comparison to the other 2DOF controls. While the data-driven planner aids in robustness, it is also advantageous compared to other planning approaches because it does not need to replan and regenerate the reference trajectory at every sampling time instant [8]. Since the action reference parameter is calculated nearly at the same rate as the feedback control, the planning process is adjusted rapidly, which enables the planner to handle unexpected disturbances within one control execution sampling time.

This paper is organized as follows. Dynamics modeling of the microdevice is introduced in Section II. The data-driven 2DOF control mechanism is discussed in Section III-V. Computer simulation is conducted in Section VI. Conclusions and future work are discussed in the final section.

2 Dynamics modeling

2.1 The micropump

The piezoelectric diaphragm displacement pump can be modeled as follows [9],

$$\Delta Vol = \frac{3a^4(5+2\mu)(1-\mu)d_{13}V_0}{4h^2(3+2\mu)}, \quad (1)$$

where ΔVol is the volume change and V_0 is the voltage applied to the lead zirconate titanate film with piezoelectric coefficient $d_{13} = 3 \times 10^{-10} m/N$ and Poisson's ratio $\mu = 0.3$. The thickness and the radius of the membrane are h and a , respectively.

Papers [10] and [11], demonstrated that the flow rate increases linearly at low actuating frequencies. When the actuating frequency exceeds a critical value, though, the flow rate does not increase and may even decrease sharply. As a result of this electro-mechanical-fluid coupling, the membrane deflects in an undesirable way at high frequencies[12].

If a voltage signal with changing polarity drives the micropump, then the flow rate can be approximated as a linear function with respect to the voltage and the actuating frequency at low frequencies.

$$Q_{pump}(V_0, f) = 2f \Delta Vol = A_d f V_0, \quad (2)$$

where $A_d = 6a^4(5+2\mu)(1-\mu)d_{13}/4h^2(3+2\mu)$ is a constant coefficient.

If, for example, $V_0 = 1.5 V$, $a = 100 \mu m$ and $h = 10 \mu m$ then according to equation (1), we will have $\Delta Vol = 3.675 \times 10^{-3} \mu l$. Assuming that the micropump is driven at 100 Hz, equation (2) gives the pumping speed as 0.735 $\mu l/s$.

2.2 Microneedle

Microneedles are attractive for medical applications in that they are able to provide painless drug transport pathways while at the same time largely reducing the risk of infection at injection site.

The volume flow rate of a microneedle can be expressed as

$$Q_{needle} = \Delta P / R, \quad (3)$$

where ΔP is the pressure drop across the channel, and R is the channel resistance for a circular channel, where

$$R = 8\mu L / \pi r^4, \quad (4)$$

In equation (4), μ is the fluid viscosity, while L and r are the channel length and radius, respectively. We choose a straight microneedle with 100/30 μm outside/inside diameter.

Because the total resistance of a microneedle array is often smaller than the sum of the individual channel

resistances, a high needle density increases the volume flow rate as follows,

$$Q_{\text{needle}} = \Delta P / k_d R, \quad (5)$$

where k_d is the discount coefficient.

The microneedle array is not sufficiently large to allow free flow, but it is large enough not to cause significant resistance. Ma *et al.* [13] showed that for microneedles, the flow rate is nearly linear to the actuating frequency at low frequencies. As a result, it is reasonable to assume that the microneedle array does not impede the flow from the micropump.

2.3 Microsensor

One of the major glucose sensors is the amperometric sensor, which determines the solution concentration by measuring the current generated during a chemical reaction. The amperometric sensor can be modeled as follows [14]:

$$\dot{I}_{\text{sig}} = -c_2 I_{\text{sig}} + c_1 G + OS, \quad (6)$$

$$G_S = CF(I_{\text{sig}} - OS), \quad (7)$$

where G_S and G are the sensor and blood glucose level, respectively. I_{sig} is the sensor signal, CF is the calibration factor and OS is the offset current. The sensor sensitivity is characterized by the ratio of c_1 and c_2 ,

The sensor glucose model can be rewritten as

$$\begin{aligned} \dot{G}_S &= -c_2 G_S + c_1 CF \cdot G + CF(1 - c_2)OS \\ &= -\theta_1 G_S + \theta_2 G + OF, \end{aligned} \quad (8)$$

where $\theta_1 = c_2$, $\theta_2 = c_1 CF$, and $OF = CF(1 - c_2)OS$.

2.4 Glucose-insulin Kinetics

Shimoda's three-compartment model [15] can be used to describe the kinetics of either regular insulin or a monomeric insulin analog supplied as a continuous subcutaneous infusion.

$$\dot{Q}_1 = -kQ_1 + u \quad (9)$$

$$\dot{Q}_2 = -(p + o)Q_2 + kQ_1 \quad (10)$$

$$\dot{I} = -k_e(I - i_b) + pQ_2 / V_i \quad (11)$$

Here Q_1 and Q_2 stand for the insulin masses at the injection site and the intermediate site, respectively. I is the plasma insulin concentration with the basal value i_b . u is the subcutaneous insulin infusion rate. k and p are the transition rate constants, and o and k_e are degradation decay rates. The parameter V_i stands for the plasma distribution volume.

The minimal model [16] has been widely accepted as the fundamental model to describe insulin-glucose interactions:

$$\dot{G} = -XG + P_1(G_b - G) + GI \quad (12)$$

$$\dot{X} = -P_2X + P_3(I - I_b), \quad (13)$$

where G is the plasma glucose level (with basal value G_b), X is the interstitial insulin concentration, GI is the intravenous glucose uptake, P_1 is a coefficient for glucose effectiveness, and P_3 / P_2 is a measure of insulin sensitivity [16].

Combining all subsystems and letting $x_1 = S - OF / \theta_1$, $x_2 = G - G_b$, $x_3 = X$, $x_4 = I - I_b$, $x_5 = Q_2$, $x_6 = Q_1$, and $\theta_3 = p / V_i$, we have the following sixth-order nonlinear model. The meaning of the parameters are summarized in the Table I.

$$\begin{aligned} \dot{x}_1 &= -\theta_1 x_1 + \theta_2 x_2 \\ \dot{x}_2 &= -(x_2 + G_b)x_3 - P_1 x_2 + GI \\ \dot{x}_3 &= -P_2 x_3 + P_3 x_4 \\ \dot{x}_4 &= \theta_3 x_5 - k_e x_4 \\ \dot{x}_5 &= kx_6 - (p + o)x_5 \\ \dot{x}_6 &= -kx_6 + u \\ y &= x_1, \end{aligned} \quad (14)$$

subject to $0 \leq u(t) \leq 10 \text{ U/h}$ and $y(t) \geq 75 \text{ mg/dL}$.

The input $u = CV_0$ is a linear function of the applied voltage V_0 according to the arguments presented in subsections A and B. In order to simplify the presentation, let us assume $C = 1$.

TABLE 1: Physical variables in the dynamic models

Symbol	Description
$x_1(\text{mg/dL})$	sensor measured plasma glucose level
$x_2(\text{mg/dL})$	plasma glucose level
$x_3(\text{min}^{-1})$	interstitial insulin
$x_4(\text{mU/L})$	plasma insulin level
$x_5(\text{mU/Kg})$	insulin mass at intermediate site
$x_6(\text{mU/Kg})$	insulin mass at the injection site
$P_1(\text{min}^{-1})$	glucose effectiveness
$P_3/ P_2(\text{L/ mU})$	insulin sensitivity
$V_i(\text{L/Kg})$	plasma distribution volume
$u(\text{mU/Kg/min})$	insulin infusion rate
$G_b(\text{mg/dL})$	basal plasma glucose level
$i_b(\text{mU/L})$	basal plasma insulin level
OF	calibration factor
OS	offset current
c_1/ c_2	sensor sensitivity

Consider a class of nonlinear systems

$$\dot{x} = f(x, u) \quad (15)$$

$$y = h(x) \quad (16)$$

with state $x \in R^n$, input $u \in R^m$ and output $y \in R^m$. In equations (15)-(16), we assume that the vector field $f(x, u)$ and the function $h(x)$ are smooth.

The glucose control problem is to regulate the blood glucose concentration from a high level to the basal level. Exact feedback linearization based nonlinear controls [17] can have good performance, however, these methods are sensitive to model uncertainties and disturbances, which is a big issue in glucose control problem. As a result, we will apply exact feedforward linearization technique based on differential flatness, which is more robust to the feedback linearization[18]. The feedforward linearization problem is to design a control u_d to track a smooth reference trajectory connecting two stationary setpoints (u_d^0, x_d^0, y_d^0) and (u_d^T, x_d^T, y_d^T) within a finite time interval $t \in [0, T]$. The control and state variables satisfy the following relationships

$$(u_d^0, x_d^0): f(x_d^0, u_d^0) = 0, y_d^0 = h(x_d^0), \quad (17)$$

$$(u_d^T, x_d^T): f(x_d^T, u_d^T) = 0, y_d^T = h(x_d^T). \quad (18)$$

2.5 Differential flatness

Definition [19, 20]: A system is said to be differentially flat if there exists a set of m differentially independent variables, $z = [z_1, \dots, z_m]^T$ such that

$$z = \mathcal{C}(x, u, \dot{u}, \dots, u^{(\beta)}), \quad (19)$$

$$x = \mathcal{A}(z, \dot{z}, \dots, z^{(\alpha)}), \text{ and} \quad (20)$$

$$u = \mathcal{B}(z, \dot{z}, \dots, z^{(\alpha+1)}), \quad (21)$$

where \mathcal{A} , \mathcal{B} , and \mathcal{C} are smooth functions of their arguments at least in an open subset of $R^{n+m(\beta+1)}$, $R^{m(\alpha+1)}$, and $R^{m(\alpha+2)}$, respectively. A vector z which satisfies the above equations is called a flat output, and then the output vector can be written with respect to the flat output,

$$y = h(x) = h(\mathcal{A}(z, \dot{z}, \dots, z^{(\alpha)})). \quad (22)$$

All flat systems can be transformed into a normal form

$$\begin{aligned} \dot{\xi}_1 &= \xi_2 \\ &\vdots \\ \dot{\xi}_{r_i-1} &= \xi_{r_i} \\ \dot{\xi}_{k_i} &= \alpha_i(\xi, u, \dot{u}, \dots, u^{(\sigma_i)}), \text{ for } i = 1, \dots, m \end{aligned} \quad (23)$$

via the Brunovsky state [21]:

$$\xi = (\xi_1^1, \xi_2^1, \dots, \xi_{r_1}^1, \xi_1^2, \dots, \xi_{r_2}^2, \dots, \xi_1^m, \dots, \xi_{r_m}^m)^T, \quad (24)$$

where $\sum_{i=1}^m r_i = n$.

By Delaleau and Rudolph [21], for the set of algebraic equations

$$\alpha_i(\xi, u, \dot{u}, \dots, u^{(\sigma_i)}) = v_i \quad (25)$$

there always exists a solution

$$u = \Theta(\xi, v, \dot{v}, \dots, v^{(\sigma)}), \quad (26)$$

where $v = [v_1, \dots, v_m]^T$ and $\sigma = \max(\sigma_i)$.

For example, consider a MIMO system

$$\dot{x}_1 = x_2 + u_1 \quad (27)$$

$$\dot{x}_2 = x_3 + x_1 u_1 \quad (28)$$

$$\dot{x}_3 = x_2 + u_2. \quad (29)$$

Set the Brunovsky state: $\xi = (x_1, x_2, \dot{x}_2)$. Then the MIMO system can be transformed into

$$\dot{\xi}_1^1 = \xi_2^1 + u_1 \quad (30)$$

$$\dot{\xi}_2^2 = \xi_2^1 + \xi_2^1 u_1 + u_1^2 + \xi_2^1 \dot{u}_1 + u_2. \quad (31)$$

As a result,

$$u_1 = \dot{\xi}_1^1 - \xi_2^1 \quad (32)$$

$$u_2 = \dot{\xi}_2^2 - \xi_1^1 (\dot{\xi}_1^1 - \xi_2^1) - \xi_1^1 (\dot{\xi}_1^1 - \xi_2^1). \quad (33)$$

In fact, differential flatness is equivalent to dynamic feedback linearization on an open and dense set using a class of invertible dynamic feedbacks [20]. For SISO systems, a differentially flat system is equivalent to a static feedback linearizable system [22]. Fliess *et al.* [20] has proved that a flat system is controllable.

Hagenmeyer and Delaleau [18] showed that if the desired trajectory is in close proximity to the initial condition x_0 , i.e.,

$$\|x_0 - \mathcal{A}(z_d, \dot{z}_d, \dots, z_d^{(\sigma)})\| < \delta, \quad (34)$$

then after applying the exact feedforward linearization control

$$u = \Theta(\xi_d, v_d, \dot{v}_d, \dots, v_d^{(\sigma)}), \quad (35)$$

the MIMO nonlinear system (23) is equivalent to the Brunovsky normal form (Proposition 1, [18]).

$$\begin{aligned} \dot{\zeta}_{r_i-1}^j &= \zeta_{r_i}^j \\ \dot{\zeta}_{r_i}^j &= \zeta_{dr_i}^j \end{aligned} \quad (36)$$

2.6 Two degree-of-freedom Control

As shown in Fig. 2, the 2DOF controllers contain two components: feedforward control providing nominal input, and feedback control ensuring stability. The addition of feedforward controllers can improve the tracking performance when compared with the use of feedback controllers alone under acceptable model uncertainties, and thereby, significantly shorten the regulating time. However, model-based feedforward controllers alone cannot resist large model

uncertainties[23], feedback controllers have been employed in conjunction with feedforward to reduce uncertainty-caused errors, such as sliding mode control [24], backstepping control[25], and PID control [18]. In this paper, we propose a 2DOF controller described as follows:

$$u = \Theta(\xi_d, v_d, \dot{v}_d, \dots, v_d^{(\sigma)}) + K(\xi)(\xi - \xi_d), \quad (37)$$

where $K(\xi)$ is a scheduled gain. The gain scheduling control is designed to compensate unknown model uncertainties and avoid singularity problem, which often occur when using linearization techniques [26, 27]. Several gain scheduling methods[8] can be chosen dependent on the system requirements. These include hard switching, linear interpolation, and switching with hysteresis.

The 2DOF method improves the robustness of the conventional feedback linearization[17], which is very sensitive to model uncertainties. The feedback linearization technique exactly cancels nonlinearities via state feedback, while the 2DOF control method uses exact feedforward linearization (35), which is known to be more robust than feedback linearization in terms of model uncertainties[18].

In the next section, a data-driven planning technique will be presented to further improve robustness towards both model uncertainties and unexpected disturbances.

3 Data-driven Planner

The 2DOF control can have better tracking performance than the use of feedback control alone in the presence of acceptable model uncertainties.[7] In reality, model uncertainties and unexpected disturbances can be large and result in substantial deviation of the output trajectory from the predefined planning trajectory. The time-driven 2DOF control often deteriorates this deviation, since the time-driven planner cannot stop, but instead continues to gives offline-computed values as time evolves. This fact will lead to poor performance, and even instability. The data-driven planner, however, refers to the current output and the planning trajectories 'stop' and 'wait' the system recovered from the disturbances. As a result, the data-driven 2DOF controller will not deteriorate the substantial deviation created by the model uncertainties or disturbances.

As shown in equation (17)-(18), we need plan a sufficiently smooth reference trajectory connecting an

initial setpoint and a terminal setpoint in the time interval T , and then use this trajectory to develop a exact feedforward linearization control (35). The sufficiently smooth reference trajectory (Fig. 3 the dotted curve) can be constructed using a polynomial series [28] as follows,

$$y_d(t) = y_0 + (y_T - y_0) \sum_{j=r+1}^{2r+1} a_j (t/T)^j, t \in [0, T], \quad (38)$$

where r is the relative degree [17] of the nonlinear system (15)-(16), and

$$a_j = \frac{(-1)^{j-(r+1)}(2r+1)!}{j \cdot r!(j-(r+1))!(2r+1-j)!}, j = r+1, \dots, 2r+1. \quad (39)$$

Alternatively, we can use an exponential function (Fig. 3 the solid curve),

$$y = (y_0 - y_T)(t/b + 1)e^{-t/b} + y_T, \quad (40)$$

where $b = T/10$.

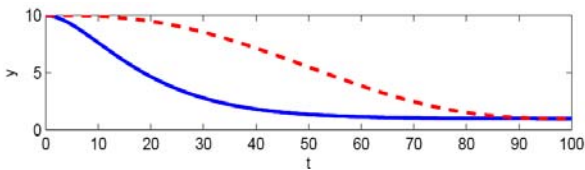


Fig. 3 Polynomial planner (dotted) v.s. Exponential planner (solid). In this illustration, we choose $T = 100$, $y_0 = 10$ and $y_T = 0$.

These reference trajectories $y_d(t)$ are sufficiently smooth, yet steep. As shown in Fig. 4(a), if an unexpected disturbance is applied over a short time period Δt , the output error $y(t) - y_d(t)$ grows sharply, as does the state error $e = x - x_d$. According to [18] and equation (34), the feedforward control u_d will fail to translate the nonlinear system into a normal form. This problem occurs because the time-driven planning trajectory refers to the reference trajectory at time instant t , i.e., $y_d(t)$. As a result, the time-driven feedforward control can have poor tracking performance, which may even lead to instability.

The data-driven planner [29, 30] is a closed-loop planner (Fig. 2) driven by an action reference, s , which is a non-time scalar factor generated by measurement data. As shown in Fig. 4(b), a simplified data-driven reference trajectory refers to the reference trajectory in

the output level, i.e., $y_d(y)$. The output error is zero and the corresponding state error is much smaller than the state error generated when using time-driven planning. As a result, the feedforward controller can guarantee good tracking performance. Theorem 1 gives a sufficient condition for stability of the data-driven control approach. Very generally, this theorem implies that the stability of data-driven control is at least the same as the stability of the time-driven control.

Moreover, in contrast to other planning approaches [8], the data-driven planner need not replan and regenerate a reference trajectory at every sampling time instant. In fact, the action reference parameter is calculated nearly at the same rate as the feedback control, meaning that the planning process is adjusted rapidly, enabling the planner to handle unexpected disturbances within one control execution sampling time.

Theorem 1 [30]: If the nonlinear system (15)-(16) is asymptotically stable with a time-driven controller $u(t)$, and the event s is monotonically increasing (or non-decreasing) with time t , i.e.,

$$ds/dt > 0 \quad (\text{or } ds/dt \geq 0), \quad (41)$$

Then this system is asymptotically stable (or stable) under the data-driven controller $u(s)$.

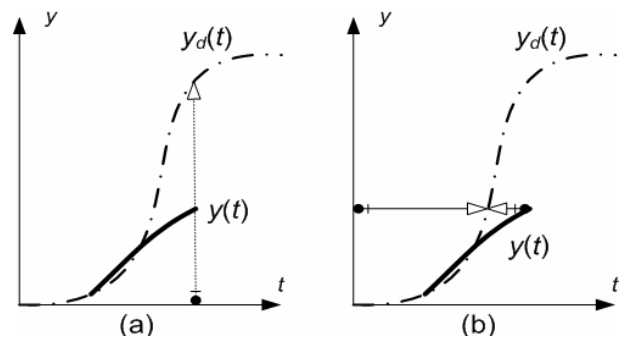


Fig. 4 Time-driven versus data-driven planning trajectory. A time-driven planning trajectory refers to the time instant t , while a data-driven planning trajectory refers to the output level y .

The data-driven planner develops a relationship between the output y and its derivatives \dot{y}, \ddot{y}, \dots , and $y^{(r)}$. The exponential reference trajectory is easier to analyze than the polynomial trajectory, although y_T can only be approximately reached in time T . Given the output y , the time t can be calculated from equation

(40) directly.

$$t/b + 1 = W, \quad (42)$$

where $W = W(-1, (y_T - y)/(y_0 - y_T)e)$ is the -1 branch of the Lambert W function, which is the solution of the function $(y_T - y)/(y_0 - y_T)e = We^W$. From these equations, the first order derivative $\dot{y}(t)$ is

$$\dot{y}(t) = (y_0 - y_T)(W + 1)e^{W+1}/b. \quad (43)$$

If the output monotonically decreases with t , the event S is defined as

$$S = y_0 - y; S_0 = 0, \quad (44)$$

Thus, the derivatives of y can be written as functions of S ,

$$\dot{y}(S) = (y_0 - y_T)(W(S) + 1)e^{W(S)+1}/b, \quad (45)$$

$$y^{(i)}(S) = -(y^{(i-2)}(S) + 2by^{(i-1)}(S))/b^2, \quad i > 2, \quad (46)$$

$$\ddot{y}(S) = -[y(S) - y_T + 2b\dot{y}(S)]/b^2, \quad (47)$$

where $W(S) = W(-1, [y_T - y(S)]/(y_0 - y_T)e)$.

Keeping in mind that the output $y(t)$ may suddenly increase because of a short unexpected disturbance, we examine the effect of this disturbance on the event S . In order to keep the monotonically nonincreasing condition required for Theorem 1, as shown in Fig. 5, the event S first increases as y decreases, but then stops evolving after y reaches a valley y_c . S resumes evolution again only after y returns to the level of y_c .

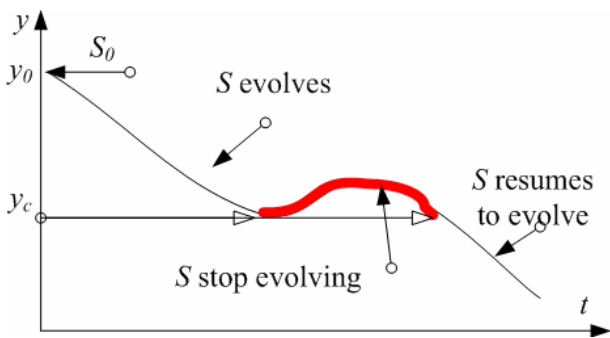


Fig. 5 The event S stops growing until y is recovered from the disturbance.

4 Control Application

In this section, we will construct flatness-based feedforward control for the insulin delivery system (14). The output is $z = x_1$, so the states can be described as functions of $z, \dots, z^{(n)}$

$$x_1 = z,$$

$$x_2 = (\tau\dot{z} + z)/\rho,$$

$$x_3 = -(\dot{x}_2 + P_1(x_2 - G_b))/x_2,$$

$$x_4 = (\dot{x}_3 + P_2x_3 + P_3i_b)/P_3,$$

$$x_5 = (\dot{x}_4 + k_e(x_4 - i_b))/V_i/p,$$

$$x_6 = (\dot{x}_5 + (p + o)x_5)/k.$$

In this case, the input also is a function of $z, \dot{z}, \dots, z^{(n-1)}$, since

$$u = \dot{x}_6 + kx_6 \quad (48)$$

Hence, the system (14) is differentially flat.

The 2DOF controller can be written as

$$u = \Theta(\xi_d) + K(z)PD(e), \quad (49)$$

where $K(z)$ is a hard-switching scheduled gain, and the state $\xi_d = [z_d, \dot{z}_d, \dots, z_d^{(n-1)}]$. The PD controller is

$$PD(e) = K_p(z - z_d) + K_d(\dot{z} - \dot{z}_d). \quad (50)$$

The feedforward control $u_d = \Theta(\xi_d)$ can be computed as

$$\bar{x}_2 = (\xi_d + \theta_1\dot{\xi}_d)/\theta_2,$$

$$D = -1/(\bar{x}_{21} + G_b),$$

$$\bar{x}_{31} = [\bar{x}_{22} + P_1\bar{x}_{21}]D,$$

$$\bar{x}_{32} = [\bar{x}_{23} + (P_1 + \bar{x}_{31})\bar{x}_{22}]D,$$

$$\bar{x}_{33} = [\bar{x}_{24} + (P_1 + \bar{x}_{31})\bar{x}_{23} + 2\bar{x}_{32}\bar{x}_{22}]D,$$

$$\bar{x}_{34} = [\bar{x}_{25} + (P_1 + \bar{x}_{31})\bar{x}_{24} + 3\bar{x}_{32}\bar{x}_{23} + 3\bar{x}_{33}\bar{x}_{22}]D,$$

$$\bar{x}_{35} = [\bar{x}_{26} + (P_1 + \bar{x}_{31})\bar{x}_{25} + 4\bar{x}_{32}\bar{x}_{24} + 6\bar{x}_{33}\bar{x}_{23} + 4\bar{x}_{34}\bar{x}_{22}]D,$$

$$\bar{x}_4 = (\bar{x}_3 + P_2\bar{x}_3)/P_3,$$

$$\bar{x}_5 = (\bar{x}_4 + k_e\bar{x}_4)/\theta_3,$$

$$\bar{x}_6 = (\bar{x}_5 + (p + o)\bar{x}_5)/k,$$

$$\Theta(\xi_d) = \bar{x}_{62} + k\bar{x}_{61}.$$

(51)

5 Simulation Results

To demonstrate the effectiveness and robustness of the data-driven 2DOF control algorithm, we test different cases by computer simulation using Matlab and Simulink. The system parameters are set as Table II.

Table 2: System Parameters Used In The Simulation

Parameters	Value	Parameters	Value
P_1	0.003082	k_e	0.267
P_2	0.02093	θ_1	0.33
P_3	0.00001282	θ_2	0.33
G_b	85	i_b	0
o	0.0125	P	0.25
k	0.25	V_i	0.21

5.1 Test of robustness

First of all, the robustness of the data-driven 2DOF control method is tested by a couple of cases.

Case 1: Various initial glucose input

Initial glucose inputs range from 5 to 40 mg/min at 6 - 11 min and the BGL(blood glucose level) is sampled every 5 min . When the data-driven 2DOF control is applied, the BGL converges to the basal level in 80 - 130 min , and remains above the minimal level. The magnitude of the insulin infusion rate grows as the initial glucose input increases. The maximum insulin infusion reaches 7 U/h , which is under the constraints.

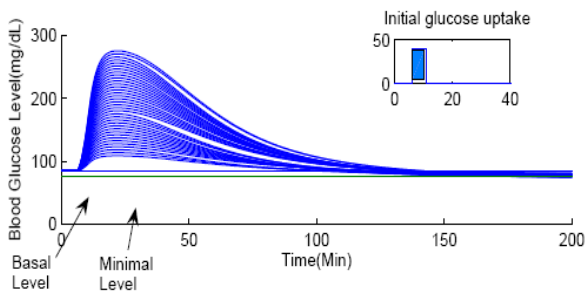


Fig. 6 The data-driven 2DOF control approach is tested by various initial glucose input, the BGL converges to the basal level in 80 - 130 min , and remains above the minimal level.

Case 2: Various sampling interval

Two glucose inputs 40 and 3 mg/min are administered at 6 - 11 min and 17 - 26 min , respectively. The BGL is

sampled from 5 to 20 min . The BGL converges to the basal level in 130 - 160 min . Clearly, the proposed method can control blood glucose levels even for a 20 min sampling interval, which would cause poor performance in most feedback-based controllers. The feedforward linearization technique in the 2DOF control largely reduces the dependence of the real-time feedback, leading to the sampling robustness observed in our simulations.

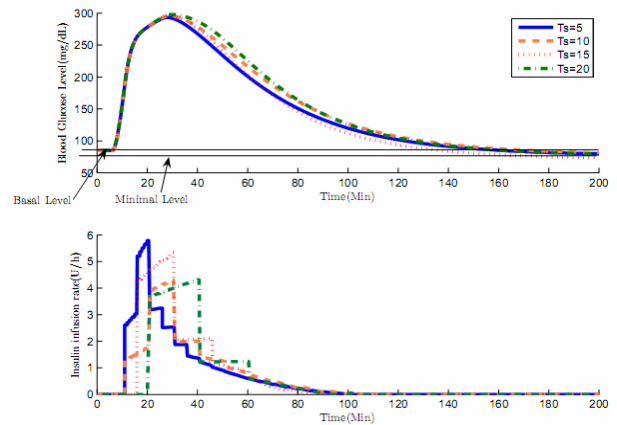


Fig. 7 The BGL is sampled from 5 min to 20 min . The BGL converges to the basal level in between 130 min and 160 min .

Case 3: model uncertainties

Two glucose inputs 40 and 3 mg/min are administered at 6 - 11 min and 17 - 26 min , respectively. The BGL is sampled every 5 min . The system (14) with model uncertainties can be written as

$$\dot{x} = f(x, u) + \delta f(x, 0), \quad (52)$$

where $\delta f(x, 0)$ implies that model uncertainties are proportional to vector field $f(x, 0)$, and $\delta > 0$ is a constant coefficient. For δ values of 0.5, 1, and 1.5, the BGL still converges under the same controller parameters. The larger model uncertainty leads to a longer convergence time; however, one can always adjust the gains of the PD controller (50) to achieve desired performance.

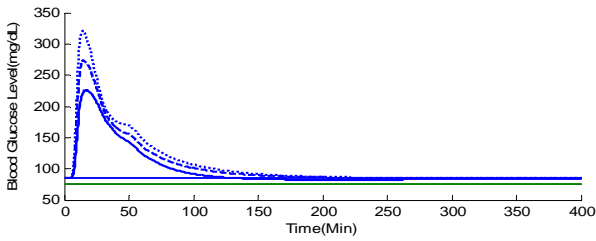


Fig. 8 The BGL converges to the basal level subject to model uncertainties. The model uncertainties are assumed to be 0.5 (solid), 1(dashed) and 1.5(dotted) times of the proposed model.

5.2 Comparing to other control algorithms

1) Time-driven approach

With a 10 mg/min initial glucose, a disturbance of 1 mg/min glucose is applied over the time period from 36 - 47 min. The data-driven approach converges to the basal level at 130 min, while the time-driven approach requires 200 min - a significant, and biologically costly delay relative to the data-driven approach.

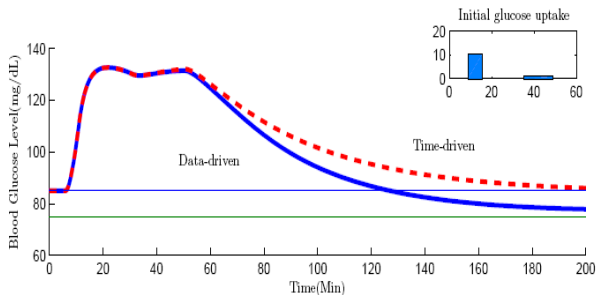


Fig. 9 In the event of disturbance, the time-driven control converges to the basal level at 200 min, while the data-driven control converges at 130 min.

2) MPC approach

The MPC (Model Predictive Control)[3, 31] is the most extensively applied control mechanism in industrial processing besides PID control. The Linear MPC approach first applies local Jacobian linearization, then uses a finite-horizon optimal control as follows,

$$\sum_{i=1}^p (y(k+i|k) - r(k+i))^T Q (y(k+i|k) - r(k+i)) + \sum_{i=1}^m u(k+i-1)^T R u(k+i-1) \quad (86)$$

Two glucose inputs 40 and 3 mg/min are administered at 6 - 11 min and 17 - 26 min, respectively. Using the MPC approach with a 5 min sampling interval, the BGL

converges to the basal level at 170 min, while the data-driven 2DOF control stabilizes the BGL at 140 min.

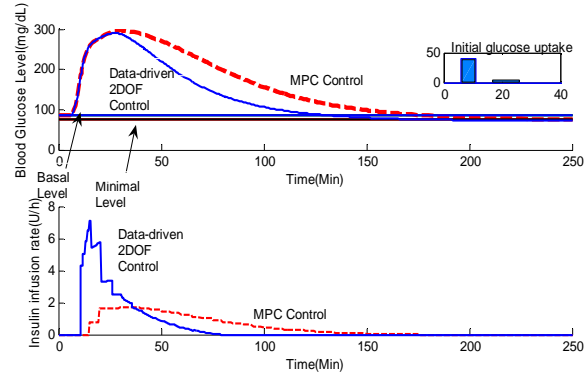


Fig. 10 BGL converges to the basal level at 170 min by MPC approach, while BGL converges at 130 min by the data-driven 2DOF control approach.

3) PD control

Two glucose inputs 20 and 3 mg/min are administered at 6 - 11 min and 17 - 26 min, respectively. Using the classical PD approach with a 5 min sampling interval, the BGL converges to the basal level at 160 min. When the first initial glucose input changes to 40 mg/min, however, the BGL significantly undershoots the minimal allowable glucose level, which may be dangerous to the patient. For both 20 mg/min and 40 mg/min, though, the data-driven 2DOF control approach makes the BGL converge at 140 min while at the same time remaining will within the safety range.

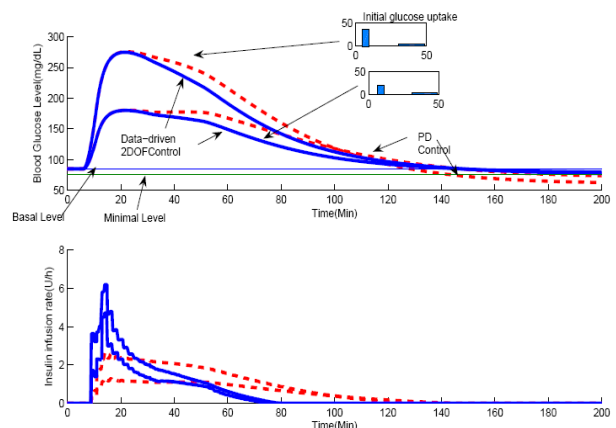


Fig. 11 Using the data-driven 2DOF control approach, the BGL converges at 140 min and above the minimal level in both cases, while the BGL goes underneath the minimal level using the classical PD control approach.

4) Backstepping control with Extended Kalman Filter
Yang *et al.* [6] proposed a backstepping control algorithm for the glucose control problem. Two glucose inputs 20 and 3 mg/min are administered at 6 - 11 min and 17 - 26 min, respectively. When we apply the classical backstepping control approach with a 5 min sampling interval and given full state information, we find that the BGL converges to the basal level at 150 min, which is comparable with our proposed approach. However, when EKF (Extended Kalman Filter) [32] is applied to estimate the states, the BGL goes underneath the minimal allowable level.

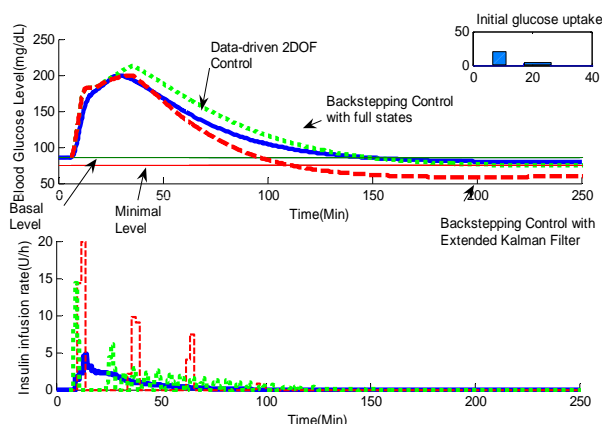


Fig. 12 Using the backstepping control approach with full states information, the BGL converges to the basal level at 150 min, similar to the data-driven approach. However, when EKF is used to estimate the states, the BGL goes underneath the minimal level.

6 Conclusions

A new data-driven 2DOF control mechanism for controlling a micropump and microneedle integrated device is presented in this paper. Compared with several feedback techniques in literature, this approach demonstrates much shorter regulating time for glucose control. In addition, this method also resists more model uncertainties and unexpected disturbances than other 2DOF controls, while has the same regulation performance. This work focuses on theoretical breakthrough and validation by computer simulation. Laboratory experiments will be implemented in future work.

ACKNOWLEDGMENT

This material is based upon work supported by the

National Science Foundation under Grant No. 0328378. The authors are grateful to the Associate Editor and to the anonymous reviewers for their valuable criticisms and suggestions, and to Dr. Sharon Bewick for many useful suggestions.

REFERENCES

- [1] G. M. Steil, K. Rebrin, J. Mastrototaro, B. Bernaba, and M. F. Saad: 'Determination of Plasma Glucose During Rapid Glucose Excursions with a Subcutaneous Glucose Sensor,' *Diabetes Technology & Therapeutics*, 2003, 5, pp. 27-31
- [2] G. Marchetti, M. Barolo, L. Jovanovic, H. Zisser, and D. E. Seborg: 'An Improved PID Switching Control Strategy for Type 1 Diabetes,' *IEEE Transactions on Biomedical Engineering*, 2008, 55, pp. 857-865
- [3] R. Hovorka, V. Canonico, L. J. Chassin, U. Haueter, M. Massi-Benedetti, M. O. Federici, T. R. Pieber, H. C. Schaller, L. Schaupp, T. Vering, and M. EWilinska: 'Nonlinear model predictive control of glucose concentration in subjects with type 1 diabetes,' *Physiol. Meas.*, 2004, 25 pp. 905-920
- [4] S. M. Lynch and B. W. Bequette: 'Model predictive control of blood glucose in type I diabetics using subcutaneous glucose measurements,' *Proc. American Control Conference*, 2002, pp. 4039-4043
- [5] F. Chee, A. V. Savkin, T. L. Fernando, and S. Nahavandi: 'Optimal H_{∞} Insulin Injection Control for blood glucose regulation in Diabetic patients,' *IEEE Transactions on Biomedical Engineering*, 2005, 52, pp. 1625 - 1631
- [6] R. Yang, M. Zhang, and T. J. Tarn, 'Control Mechanisms for Life Science Automation,' in *Life Science Automation: Fundamentals and Applications*, M. Zhang, B. Nelson, and R. A. Felder, Eds.: Artech House Publishers, 2007.
- [7] S. Devasia: 'Should model-based inverse inputs be used as feedforward under plant uncertainty?,' *IEEE Trans. on Automatic Control*, 2002, 47, pp. 1865-1871
- [8] M. van Nieuwstadt: 'Trajectory Generation for Nonlinear Control Systems,' California Institute of Technology, 1996.
- [9] D. L. Polla, A. G. Erdman, W. P. Robbins, D. T. Markus, J. Diaz-Diaz, R. Rizq, Y. Nam, H. T. Brickner, A. Wang, and P. Krulevitch: 'Microdevices in Medicine,' *Annual Review of Biomedical Engineering*, 2000, 2, pp. 551-576
- [10] N. T. Nguyen and X. Huang: 'Miniature valveless pumps based on printed circuit board technique,' *Sensors Actuators A* 2001, 88 pp. 104-11
- [11] T. Gerlach and H. Wurmus: 'Working principle and performance of the dynamic micropump,' *Sensors Actuators A* 1995, 50, pp. 135-40
- [12] B. Fan, G. Song, and F. Hussain: 'Simulation of a piezoelectrically actuated valveless micropump,' *Smart Mater. Struct.*, 2005, 14, pp. 400-405
- [13] S. A. Ramsey, J. J. Smith, D. Orrell, M. Marelli, T. W. Petersen, P. de Atauri, H. Bolouri, and J. D. Aitchison: 'Dual feedback loops in the GAL regulon suppress cellular heterogeneity in yeast,' *Nature Genetics*, 2006, 38, pp. 1082-1087
- [14] G. M. Steil, A. E. Panteleon, and K. Rebrin: 'Closed-loop insulin delivery - the path to physiological glucose control,' *Advanced Drug Delivery Reviews*, 2004, 56, pp. 125-144
- [15] S. Shimoda, K. Nishida, M. Sakakida, Y. Konno, K. Ichinose, M. Uehara, T. Nowak, and M. Shichiri: 'Closed-loop subcutaneous insulin infusion algorithm with a short-acting insulin analog for long-term clinical application of a wearable artificial endocrine pancreas,' *Frontiers Medical Biological engineering*, 1997, 8, pp. 197-211
- [16] R. N. Bergman, L. S. Phillips, and C. Cobelli: 'Physiologic evaluation of factors controlling glucose tolerance in man,' *Journal of Clinical Investigation*, 1981, 68, pp. 1456-1467
- [17] A. Isidori: *Nonlinear Control Systems* (Springer, New York 1989)

- [18] V. Hagenmeyer and E. Delaleau: 'Exact feedforward linearization based on differential flatness,' *International J. Control*, 2003, 76, pp. 537-556
- [19] M. Fliess, J. Levine, P. Martin, and P. Rouchon: 'Flatness and defect of nonlinear systems: introductory theory and examples,' *International J. Control*, 1995, 61, pp. 1327-1361
- [20] M. Fliess, J. Levine, P. Martin, and P. Rouchon: 'A Lie-Backlund approach to equivalence and flatness of nonlinear systems,' *IEEE Trans. on Automatic Control*, 1999, 44, pp. 922-937
- [21] E. Delaleau and J. Rudolph: 'Control of flat systems by quasi-static feedback of generalized states,' *International Journal of Control*, 1998, 71, pp. 745-765
- [22] M. van Nieuwstadt, M. Rathinam, and R. M. Murray: 'Differential Flatness and Absolute Equivalence of Nonlinear Control Systems,' *J. Control and Optimization*, 1998, 36, pp. 1225-1239
- [23] Y. Zhao and S. Jayasuriya: 'Feedforward controllers and tracking accuracy in the presence of plant uncertainties,' *Proc. American Control Conference, 1994*, 1994, pp. 360-364 vol.1
- [24] H. Sira-Ramirez, "Sliding mode control of the PPR mobile robot with a flexible join," in *Nonlinear Control in the Year 2000*. vol. 259 London: Springer, 2000, pp. 421-442.
- [25] P. Martin, R. M. Murray, and P. Rouchon, "Flat systems, equivalence and feedback," in *Advances in the Control of Nonlinear Systems*. vol. 264 London: Springer, 2000, pp. 5-32.
- [26] R. Yang, M. Zhang, and T. J. Tarn: 'Dynamic Modeling and Control of a Micro-needle Integrated Piezoelectric Micro-pump for Diabetes Care,' *Proc. IEEE Conference on Nanotechnology*, Cincinnati, USA, 2006
- [27] F. Doyle III, J. Harting, C. Dorski, and N. Peppas: 'Control and modeling of drug delivery devices for the treatment of diabetes,' *Proc. American Control Conf*, Seattle, WA, 1995, pp. 776-780
- [28] A. Piazzi and A. Visioli: 'Optimal Inversion-Based Control for the Set-Point Regulation of Nonminimum-Phase Uncertain Scalar,' *IEEE Transactions On Automatic Control*, 2001, 46, pp. 1654-1659
- [29] T. J. Tarn, N. Xi, and A. K. Bejczy: 'Path-Based Approach to Integrated Planning and Control for Robotic System,' *Automatica*, 1996, 32,
- [30] N. Xi and T. J. Tarn: 'Stability analysis of non-time referenced internet - based telerobotic systems,' *Robotics and Autonomous Systems*, 2000, 32, pp. 173-178
- [31] R. S. Parker, F. J. Doyle III, and N. A. Peppas: 'A model-based algorithm for blood glucose control in type I diabetic patients,' *IEEE Transactions on Biomedical Engineering* 1999, 46, pp. 148-157
- [32] M. Boutayeb and D. Aubry: 'A strong tracking extended Kalman observer for nonlinear discrete-time systems,' *IEEE Transactions on Automatic Control*, 1999, 44, pp. 1550-1556